Modulation of Twin Tropical Cyclogenesis by the MJO Westerly Wind Burst during the Onset Period of 1997/98 ENSO

ZHU Congwen*[1,3] (祝从文), Tetsuo NAKAZAWA[2], and LI Jianping[3] (李建平)

[1] *Chinese Academy of Meteorological Sciences, Beijing* 100081

[2] *Meteorological Research Institute, Tsukuba, Japan* 305-0051

[3] *LASG, Institute of Atmospheric Physics, Chinese Academy of Sciences, Beijing* 100029

(Received 31 December 2002; revised 9 April 2003)

ABSTRACT

The modulation of twin tropical cyclogenesis in the Indian-western Pacific Oceans by the Madden-Julian Oscillation (MJO) during the onset period of 1997/98 ENSO is explored for the period of September 1996 to June 1997 based on daily OLR, NCEP/NCAR wind vector, and JTWC best track datasets. The MJO westerly wind burst associated with its eastward propagation can result in a series of tropical cyclogeneses in a multi-day interval. Only in the transition seasons are pairs of tropical cyclones observed in both the tropical sectors of the Indian-western Pacific Oceans. Two remarkable twin tropical cyclogeneses probably modulated by the MJO westerly wind burst are found: one is observed in the Indian Ocean in the middle of October 1996, and the other is observed in the Western Pacific Ocean in late May 1997. The twin tropical cyclogenesis in mid-October 1996 is observed when the super cloud cluster separates into two isolated clusters by the enhanced westerly wind, which is accompanied by two independent vortices in the equatorial tropical sectors. The other one, in late-May 1997, however, is characterized by one cyclonic flow that later results in another cyclonic cell in its opposite equatorial sector. Thus, there are two very important conditions for twin cyclogenesis: one is the MJO westerly wind straddling the equator, and the other is the integral super cloud cluster, which later splits into two cloud convective clusters with independent vortices.

Key words: Madden-Julian oscillation, westerly wind burst, twin tropical cyclogenesis

1. Introduction

The Madden-Julian Oscillation (MJO), characterized by eastward propagating tropical convective anomalies and associated with circulation anomalies, has a time period between 30 to 60 days (Murakami et al., 1986; Knutson and Weickmann, 1987; Nakazawa, 1988; Rui and Wang, 1990; Li and Wu, 1990; Kiladis and Weickmann, 1992; Madden and Julian, 1994). As a dominant mode of intraseasonal variability in the tropical atmosphere with periods of 30–60 days in character, the MJO has been extensively studied since it was first observed by Madden and Julian (1971). Studies suggest that the MJO has a baroclinic, mixed Kelvin and Rossby wave structure in the Indian and the western Pacific Oceans, where the equatorial wave is strongly coupled to convection with eastward propagation in convection at roughly $5\,\mathrm{m\,s^{-1}}$. Kelvin waves propagate eastward out of the convective regions at phase speeds of 10–$12\,\mathrm{m\,s^{-1}}$ (Hendon and Salby, 1994), and are generally manifested as an eastward propagating, equatorially-trapped, wave number one, baroclinic oscillation in the tropical wind field (Madden and Julian, 1994). A hierarchy of convective organization has been observed within the wet phase of the MJO, with eastward propagating super cloud clusters with diameters of several thousand kilometers forming an envelope of enhanced mesoscale cloud cluster activity in eastward/westward motions (Nakazawa, 1988; Hendon and Liebmann, 1994).

Many studies have addressed the modulation of tropical cyclogenesis by the MJO. Earlier study has found that the tropical cyclogenesis is not evenly distributed in time within any particular season (Gray, 1979). Most of the tropical cyclones in the western

*E-mail: tomzhu@cams.cma.gov.cn

Pacific have formed during the active phase of the intraseasonal variations (Nakazawa, 1986), and the increases and decreases in numbers of tropical cyclogeneses are consistent with the phase of wet and dry MJO (Liebmann et al., 1994; Maloney and Hartmann, 1999, 2000; Hall et al., 2001). When MJO wind anomalies in the lower troposphere of the eastern Pacific are westerly, the Gulf of Mexico and western Caribbean hurricane genesis is four times more likely than when the MJO winds are easterly (Maloney and Hartmann, 2000). In additional, the twin cyclone formation is closely related with the MJO westerly wind burst. Ogura and Chin (1987) demonstrated an example of the twin cyclone originating from the equatorial enhanced convection. Twin cyclones closer to the equatorial region in the western Pacific were simulated associated with the MJO westerly wind burst (Lau et al., 1989; Chao and Deng, 1998).

Although a number of observational and modeling studies have suggested that MJO has a strong effect on tropical cyclogenesis, few works can be found on the discussion of tropical depression (TD) and tropical cyclone (TC) activities in both equatorial tropical regions, where the two hemisphere TCs are probably modulated by MJO. Whether each of the MJO convective anomalies, along with the westerly wind burst, would result in twin tropical cyclones formation has not been well explored in the previous observational studies. Following the way of Hall et al. (2001) and based on the previous work of Nakazawa (2000a, b), the purposes of this study are to investigate the modulation of twin tropical cyclogenesis by MJO westerly wind burst in the Indian-western Pacific regions in both hemispheres during the onset period of the 1997/98 ENSO. The data and methods of the present study are introduced in section 2, tropical cyclogenesis possibly modulated by MJO will be discussed in section 3, and section 4 is the conclusion.

2. Data and methodology

2.1 *Datasets*

The best track of TD/TC data set in the domain of the Indian-western Pacific Ocean is produced by the Joint Typhoon Warning Center (JTWC), Pearl Harbor, Hawaii, USA. It contains 6-hourly TD/TC position and maximum wind speed in knots. Each significant TD/TC formed in the Indian-western Pacific Oceans for the period of 1 September 1996 to 30 June 1997 is included in this study. Here, the timing and position of TD and TC are defined according to the JTWC first record with the minimum wind speed and the wind speed greater than 34 knots (nearly 17 m s^{-1}), which is used as the threshold of tropical storm genesis maximum wind speed (Zehr, 1992). It is very difficult to exactly determine the position and timing of TD/TC. Study has suggested that the JTWC observed TD and TC position has a maximum of two hundred kilometers difference compared with sea wind data based on NASA Scattrometer (NSCAT) (Nakazawa and Zhu, 2001). In the present examination, we hypothesize that the observed the position and timing of TD and TC within 200 km in error would cause less influence on our current study because of the 30–60-day large-scale MJO. The Outgoing Longwave Radiation (OLR) data is produced by the National Oceanic and Atmospheric Administration (NOAA) polar orbiting satellites. Seasonal climate variation is obtained by daily OLR for the period of November 1974 to December 2000. Wind field reanalysis datasets are from the National Centers for Environmental Prediction-National Center for Atmospheric Research (NCEP-NCAR) (Kalnay et al., 1996) and are retrieved for a similar period. Both datasets used in this study are daily means, with $2.5^\circ \times 2.5^\circ$ spatial resolution. In additional, the 3-hourly GMS IR data, with $1^\circ \times 1^\circ$ resolution for the analysis period is used in the twin cyclone analysis. For the purpose of background analysis, the U.K Meteorology Office $1^\circ \times 1^\circ$ weekly SST dataset (Reynolds, 1994) is also used in our study.

The North Indian Ocean and western North Pacific Ocean demarcated by 100°E and 135°E is used as the dividing line of the South Indian Ocean and southwestern Pacific Ocean, therefore, the Indian-western Pacific is classed into four basins in our analysis.

An El Niño-Southern Oscillation (ENSO) event occurred in 1997/98, whose onset phase partly covered the period of April to June 1997. The averaged weekly SST anomaly between 5°N to 5°S shows that the first indication for an El Niño in late April 1997 when SST anomalies shift to the Eastern Pacific, where the Nino3 SST anomaly index start to be positive. In October and November of 1997, it reaches the mature phase with more than +3°C in amplitude (Fig. 1a). There is abundant evidence which suggests TC formation is strongly modulated by the state of ENSO (Solow and Nicholls, 1990; Evans and Allen, 1992). However, a number of studies have suggested that ENSO onset is more triggered by MJO, particularly for 1997/98 ENSO (Slingo et al., 1999; McPhaden, 1999). In this present study, we hypothesize that ENSO causes less impact on tropical cyclogenesis.

During the period of September 1996 to June 1997, 71 TDs and 66 TCs occurred in the Indian-western Pacific Oceans according to the JTWC (Fig. 1b), and those TD/TCs positions exhibited two long belt-like patterns within the 25°S–25°N tropical sectors. In the

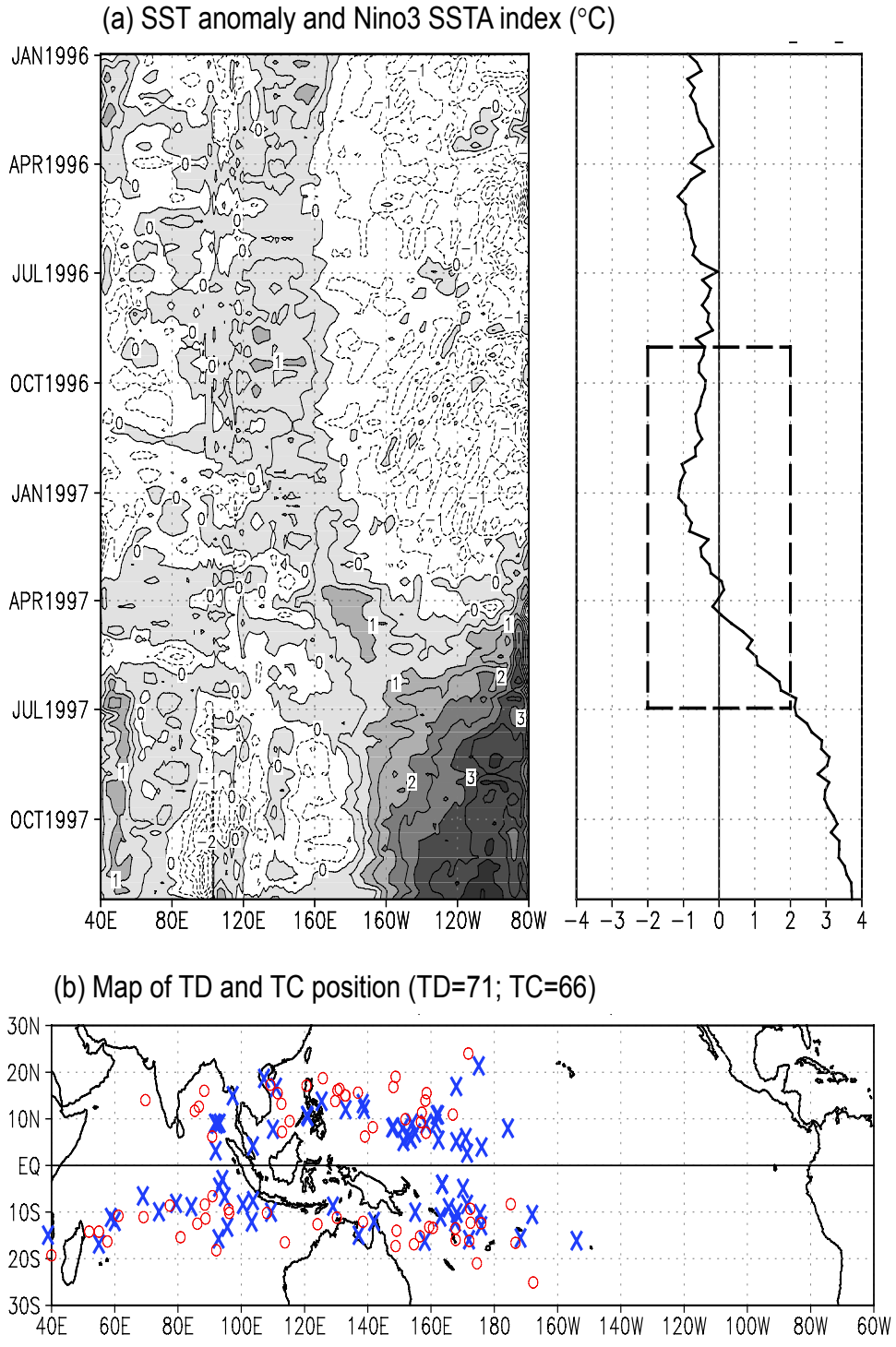

Fig. 1. (a) Time-longitude cross-section of weekly SSTA and Niño-3 SSTA index time series (°C) in the period of January 1996 to the end of December 1997. The box denotes the present study period of 1 September 1996 to 30 June 1997. (b) Map of TD/TC positions from 1 September 1996 to 30 June 1997 in the Indian-western Pacific Oceans. The cross marks denote TDs, and the TCs are marked by open circles.

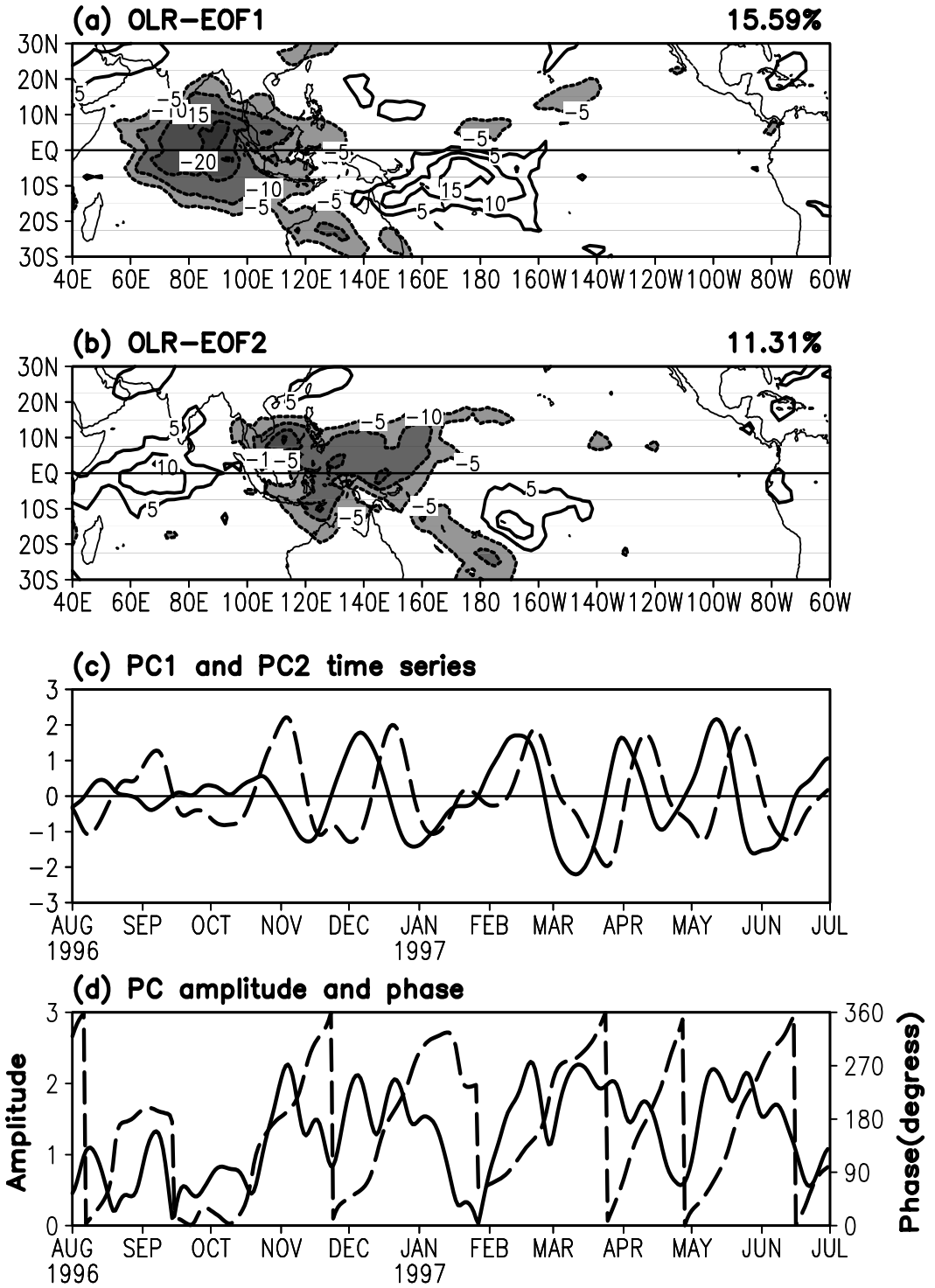

Fig. 2. Empirical orthogonal function analysis of 20–120-day filtered OLR. (a) EOF1, (b) EOF2; contour interval is 5 W m^{-2}; the zero contour is omitted; shading is shown by the legend. (c) PC1 (solid line) and PC2 (dashed line) from 1 August 1996 to 30 June 1997. (d) Phase (dashed line: scale on the right-hand axis) and daily amplitude A (solid line: scale on the left-hand axis) of $\boldsymbol{Z}$ from 1 August 1996 to 30 June 1997.

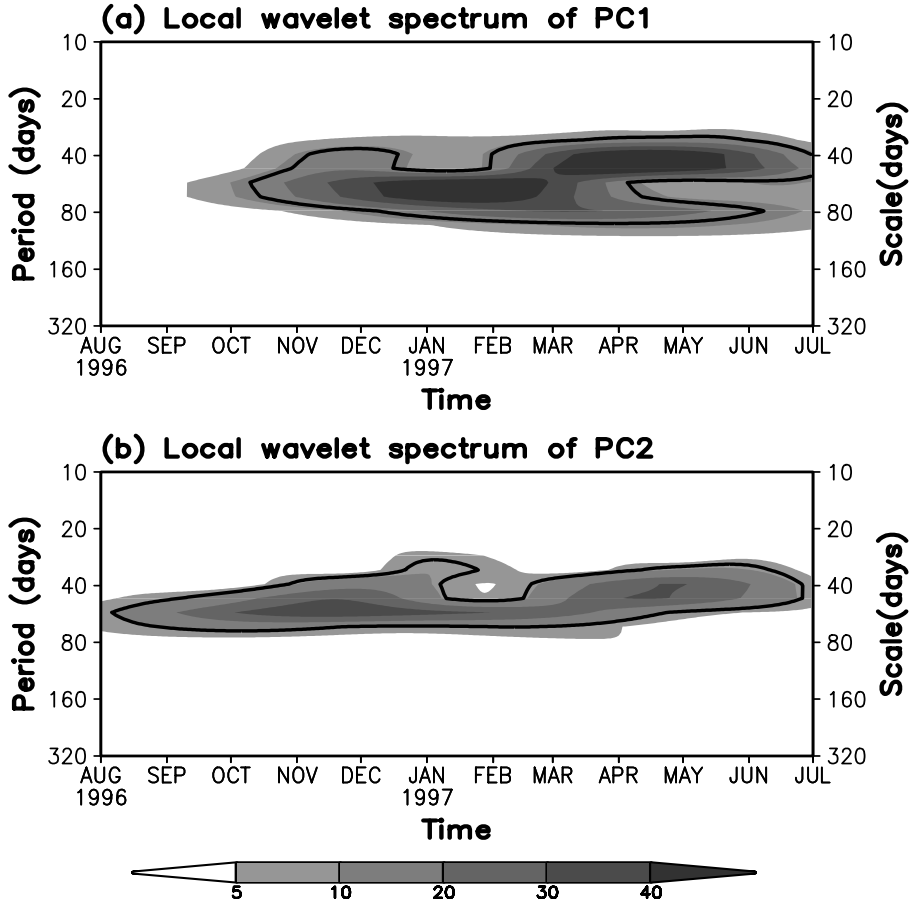

Fig. 3. Local Morelet wavelet power spectrum (unit: ×10) of (a) PC1 and (b) PC2, corresponds to the mode of EOF 1 and EOF2. The left axis is the Fourier period (day) corresponding to the wavelet scale on the right axis. The solid line encloses regions of greater than 95% confidence for a red-noise process with a lag-1 coefficient of 0.98.

North Indian Ocean, there are 5 TD/TCs, 18 TD/TCs in the South Indian Ocean, 30 TDs and 25 TCs in the western North Pacific Ocean, and 18 TD/TCs in the southwestern Pacific Ocean.

2.2 *MJO cycle and categories*

OLR, as a proxy for deep tropical convection, has been extensively used in MJO convective anomaly analysis in past studies. Recently, Matthews (2000) and Hall et al. (2001) used the Empirical Orthogonal Function (EOF) analysis of the OLR data to define the cycle of the MJO, and achieved success in separating the eastward and westward propagation of MJO. According to Matthews, the state of the MJO on any given day can be defined by the first two leading empirical orthogonal functions (EOFs) of 20–200-day filtered tropical OLR.

Following this way, but focusing on the domain of 40°E–60°W in the 30°N to 30°S tropical regions and using the 20–120-day filtered OLR data, EOF analysis is applied to OLR anomaly data. Figure 2 is the result of EOF analysis for the OLR. In the figure, the EOF1 shows the familiar MJO convective dipole, with negative OLR anomalies associated with enhanced convection over the Indian Ocean and positive OLR anomalies corresponding to reduced convection over the western Pacific (Fig. 2a). EOF2 shows enhanced convection over the Indonesian sector and along the South Pacific Convergence Zone (SPCZ), and areas of reduced convection over Africa and the central Pacific (Fig. 2b). Such EOF-based MJO modes are quite similar to the modes given by Hall et al., but more variance is explained by EOF1 and EOF2 (15.59% and 11.31% of the total variance, respectively), which makes the MJO convective anomalies quite distinguished in the Indian-western Pacific Oceans.

The MJO can be represented by the vector $\boldsymbol{Z}$ in a two-dimensional phase space, which is defined by the

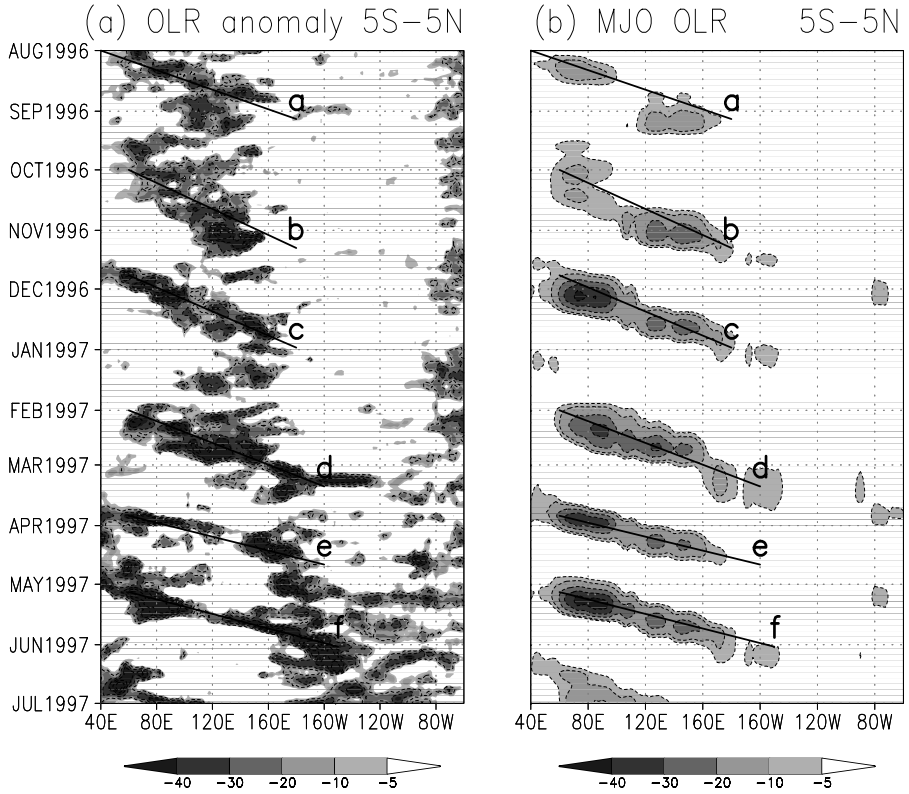

Fig. 4. Time-longitude cross-section of daily OLR anomalies and the MJO related OLR convection based on the reconstruction of two leading EOFs averaged for 5°S–5°N. (a) Daily OLR; (b) MJO-related OLR. The contour lines are –5, –10, –20, –30, and –40 W m^{-2}, the positive contours of OLR anomalies are omitted. a, b, c, d, e, and f denote each MJO event and eastward propagation.

two leading principal component time series of EOF1 and EOF2 (Matthews, 2000),

$$\boldsymbol{Z}(t) = [C_{\rm p1}(t), C_{\rm p2}(t)] \,. \tag{1}$$

Here $C_{\rm p1}$ and $C_{\rm p2}$ are the principal component time series of EOF1 and EOF2 (PC1 and PC2). The MJO amplitude is then given by

$$A(t) = [C^2_{\rm p1}(t) + C^2_{\rm p2}(t)]^{1/2} \,, \tag{2}$$

and the phase is exhibited by

$$\alpha(t) = \tan^{-1}[C_{\rm p2}(t)/C_{\rm p1}(t)] \,. \tag{3}$$

During a period of MJO activity, the principal component time series of EOF1 ($C_{\rm p1}(t)$) leads the corresponding time series for EOF2 ($C_{\rm p2}(t)$) by a quarter of an MJO cycle over the western Pacific sector; such variation of PCs suggests the eastward propagation and activity of MJO. There are six pronounced successive MJO events observed from the beginning of August 1996 to the end of June 1997 shown by the amplitude of PC1 and PC2 with PC1 leading PC2 by a quarter cycle (Fig. 2c). However, during the periods of September to early October 1996 and early January to the end of February 1997, we observe the westward propagating convective anomalies with small amplitude of $A(t)$ evidenced by the phase. and amplitude (Fig. 2d). Such westward movement is different from the typical MJO behavior (Madden and Julian, 1994); it is defined as a westward propagating MJO in contrast with the MJO eastward shift, and is placed in a non-MJO category (Hall et al., 2001).

Wavelet analysis on PC1 and PC2 shows that there are significant 30- to 60-day oscillations in PC1 and PC2 in their time series variations with a 95% confidence level. (Fig. 3). Thus, the EOF is a very effective technical tool to extract the MJO modes in temporal and spatial domains. On the basis of constructed OLR by regressing EOF1 and EOF2 spatial modes onto the PC1 and PC2 time series, the averaged longitude and time cross-section between 5°N to 5°S suggest that there are six MJO cycles which exhibit eastward propagation in their manner, individually labeled by a, b, c, d, e, and f (Fig. 4). Lag correlation between PC1 and PC2 shows that the correlation coefficient reaches

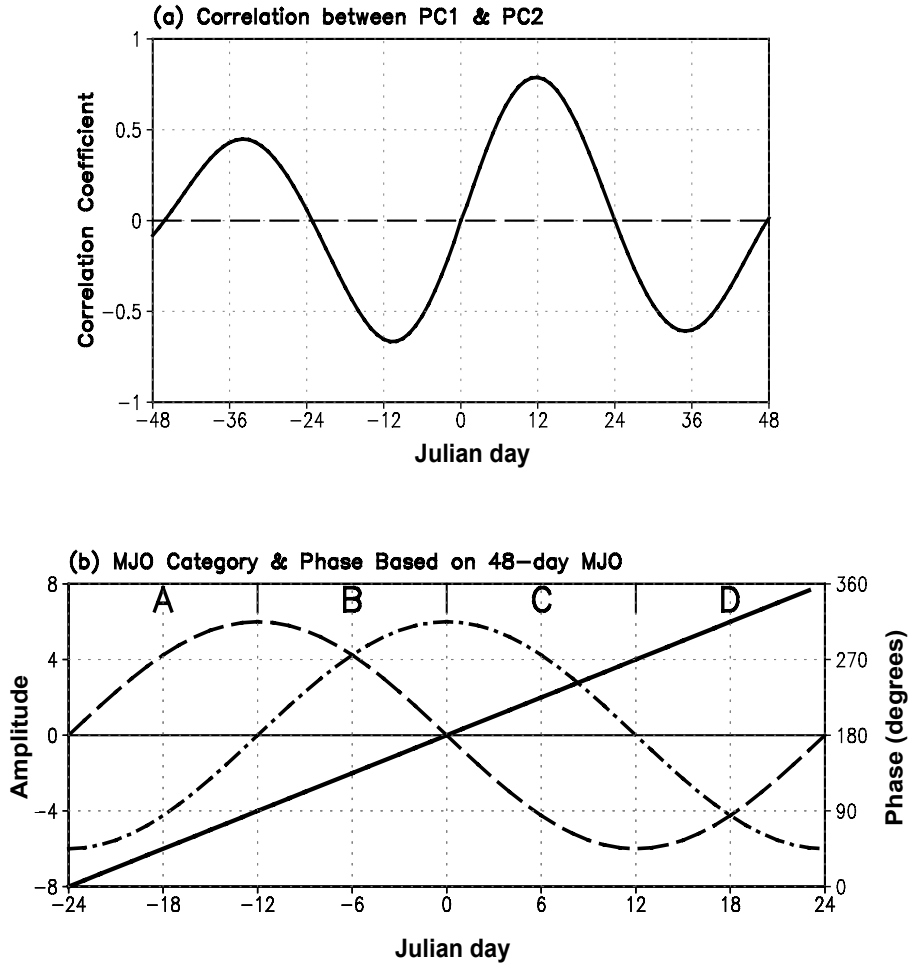

Fig. 5. Lag correlation between PC1 and PC2 and the MJO category based on a 48-day cycle of MJO. (a) Lag correlation between PC1 and PC2; (b) MJO category A, B, C, and D corresponding to the phase of α (thick solid line; scale on right-hand axis) of $\boldsymbol{Z}$ with the phase of PC1 (dashed line) and PC2 (dot-dashed line); scale on the left-hand axis.

its minimum and maximum when PC1 leads and lags PC2 by –12 day and +12 day, suggesting a quarter cycle of MJO is around 12 days, and the average MJO cycle is approximately 48 days (Fig. 5a). Following Hall et al. (2001), an MJO cycle is divided into four categories named A, B, C, and D, each covering a quarter of the MJO cycle. Category A is initially defined as those times when the phase of MJO is in the quarter cycle when $\alpha = 0°$. (Fig. 5b), around the period when PC2 is a minimum and PC1 is maximum. Similarly, categories B, C, and D are initially defined as the times when the phase is in the quarter cycles centered on α=90°, 180°, and 270°, respectively, corresponding to the times around when PC2 is a maximum, PC1 is a minimum, and PC2 is a minimum, respectively. Such a classification guarantees that each category is on the order of 12 days long, which possibly covers the life cycle of TC in any basin.

3. MJO westerly wind burst and twin tropical cyclogenesis

The low-level zonal wind at 850 hPa is used to indicate the MJO westerly wind field. To extract the mode of MJO westerly wind possibly coupled to the MJO convection, Singular Value Decomposition (SVD, Kuroda, 1998) is applied to the 20–120-day filtered OLR to the zonal wind at 850 hPa with variation trend removed.

Figure 6 shows the first couple of SVD modes and their time series. The OLR SVD mode and its time series exhibit the similar patterns we have seen in EOF1 (Fig. 6a). We can observe that accompanied with the

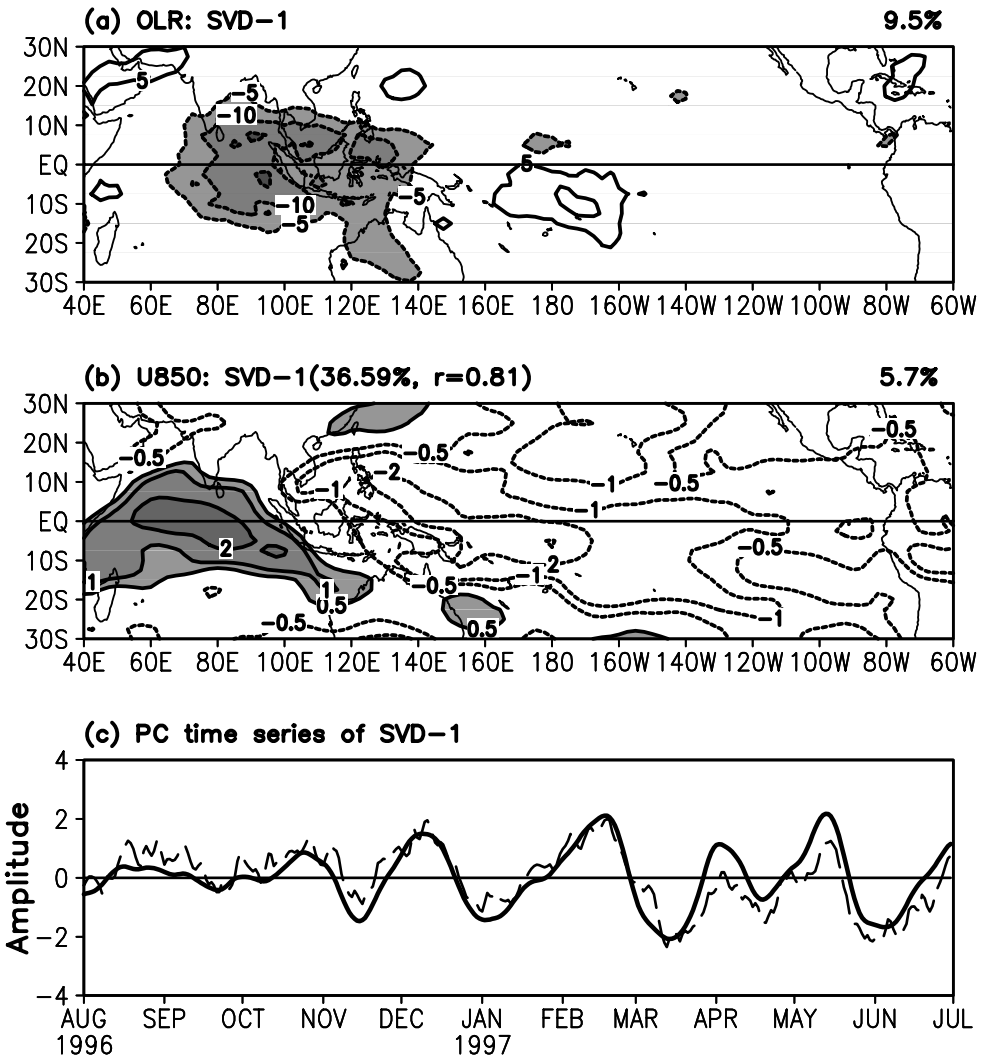

Fig. 6. Heterogeneous variance pattern for the first mode of the SVD analysis between the OLR and 850-hPa westerly wind anomalies. (a) OLR variance pattern; contour interval is 5 W m^{-2}, the zero contour is omitted. Shading is indicated by the legend; (b) 850-hPa zonal wind variance pattern; the contour interval is 1 m s^{-1}; negative contours are dotted and the zero contour is omitted. Shading is indicated by the legend. The squared covariance fraction between the two fields is expressed as a percentage and is printed in the brackets of the title; temporal correlation coefficients r is printed in the brackets as well. The percentage of variance accounting for the total are each expressed in the titles of (a) and (b). (c) Time series for the mode of OLR (solid line) and the mode of the zonal wind (dashed line) in SVD mode from 1 August 1996 to 30 June 1997.

OLR-indicated enhanced convection in the Indian Ocean, westerly wind anomalies can also be observed as well, which cover the whole equatorial Indian Ocean with the maximum amplitude centered on 70°E. The easterly wind anomalies cover the whole tropical equatorial western Pacific sectors centered on SPCZ, although there still exists convection in the western Pacific warming pool (Fig. 6b). Thus, the dipole of equator-trapped convective anomalies is always accompanied by the dipole of equatorially trapped westerly anomalies. The westerly and the easterly wind anomalies nearly cover the Indian-western Pacific regions, and meet over the Indonesian sectors, where the enhanced convection reaches its maximum amplitude. Such modes are in agreement with the patterns described by Madden and Julian (1971).

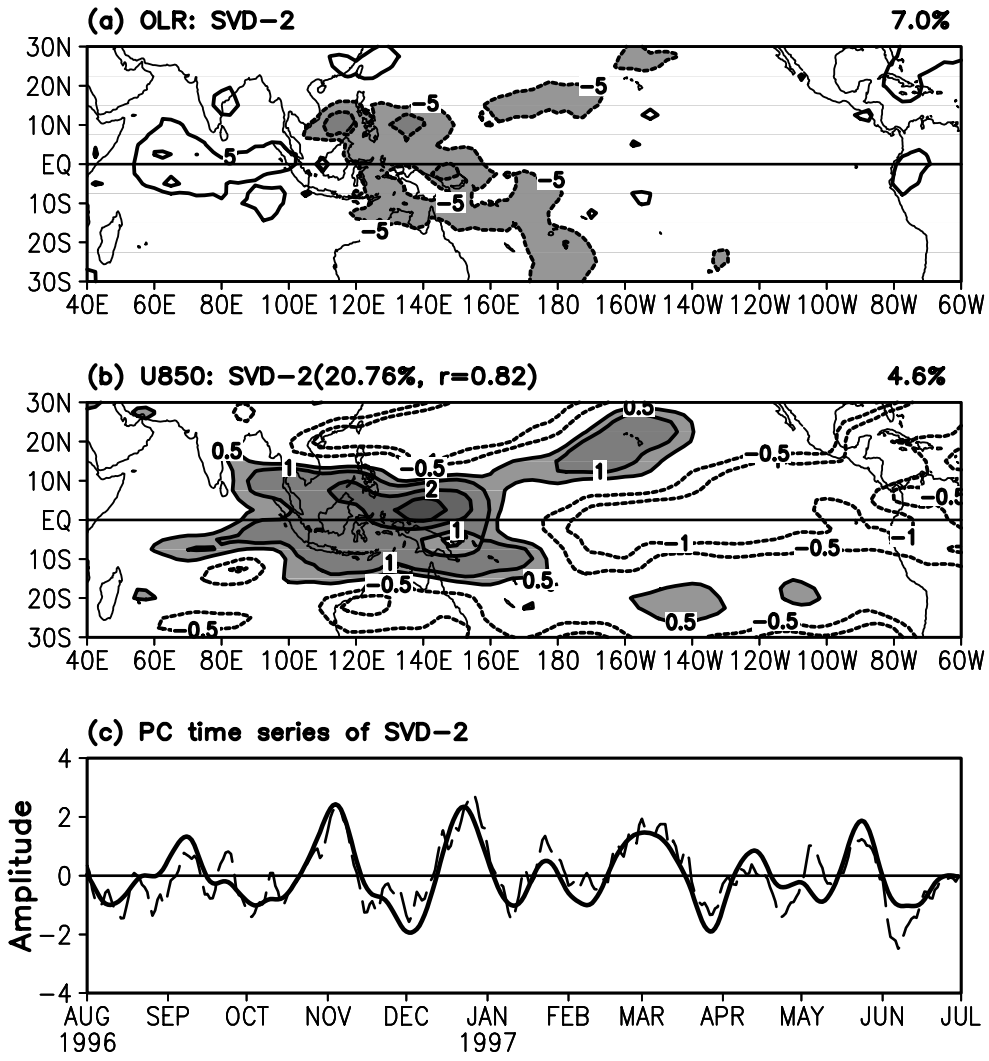

Fig. 7. Same as Fig. 6, but for the second SVD mode.

The time series of westerly wind SVD mode exhibits a wave packet manner characterized by 30- to 60-day oscillation with nested high frequency fluctuation; its time variation is in direct proportion to the convective counterpart. The second couple of SVD modes exhibit similar characteristics but the enhanced convective anomalies exist in the western Pacific where the westerly wind burst with the maximum amplitude is around 140°E (see Fig. 7). In the suppressed convective region of the equatorial eastern Pacific, we find the easterly wind anomalies, but there are no remarkable wind anomalies even when the convection in the Indian Ocean is also suppressed. Similarly, the time series of SVD modes show consistent variations in time, characterized by the 30- to 60-day cycle.

The MJO westerly wind is examined by constructing regression maps of the first two SVD modes of 850-hPa zonal winds for the different categories of MJO. Maps of anomalous westerly wind for the MJO categories are shown in Fig. 8. In category A, there is a small area of westerly anomalies straddling the equator in the Indian Ocean, corresponding to the large area of the anomalous easterly in the tropical western Pacific basin. The linkage of the equatorially trapped dipole of westerly anomalies exits in the south of the Bay of Bengal equatorial sectors, corresponding to the enhanced convection. During category B, the amplitude is enhanced and the area is enlarged, and the whole equatorial Indian Ocean is dominated by the westerly wind. The continuous eastward propagation of the westerly anomalous dipole is also observed in periods C and D, and the westerly anomaly replaces the easterly anomaly from the west. Therefore, the westerly wind burst is not a local phenomena: it originates from the Indian Ocean, and its intensity is enhanced and area enlarged step by step in the cycle of its equa-

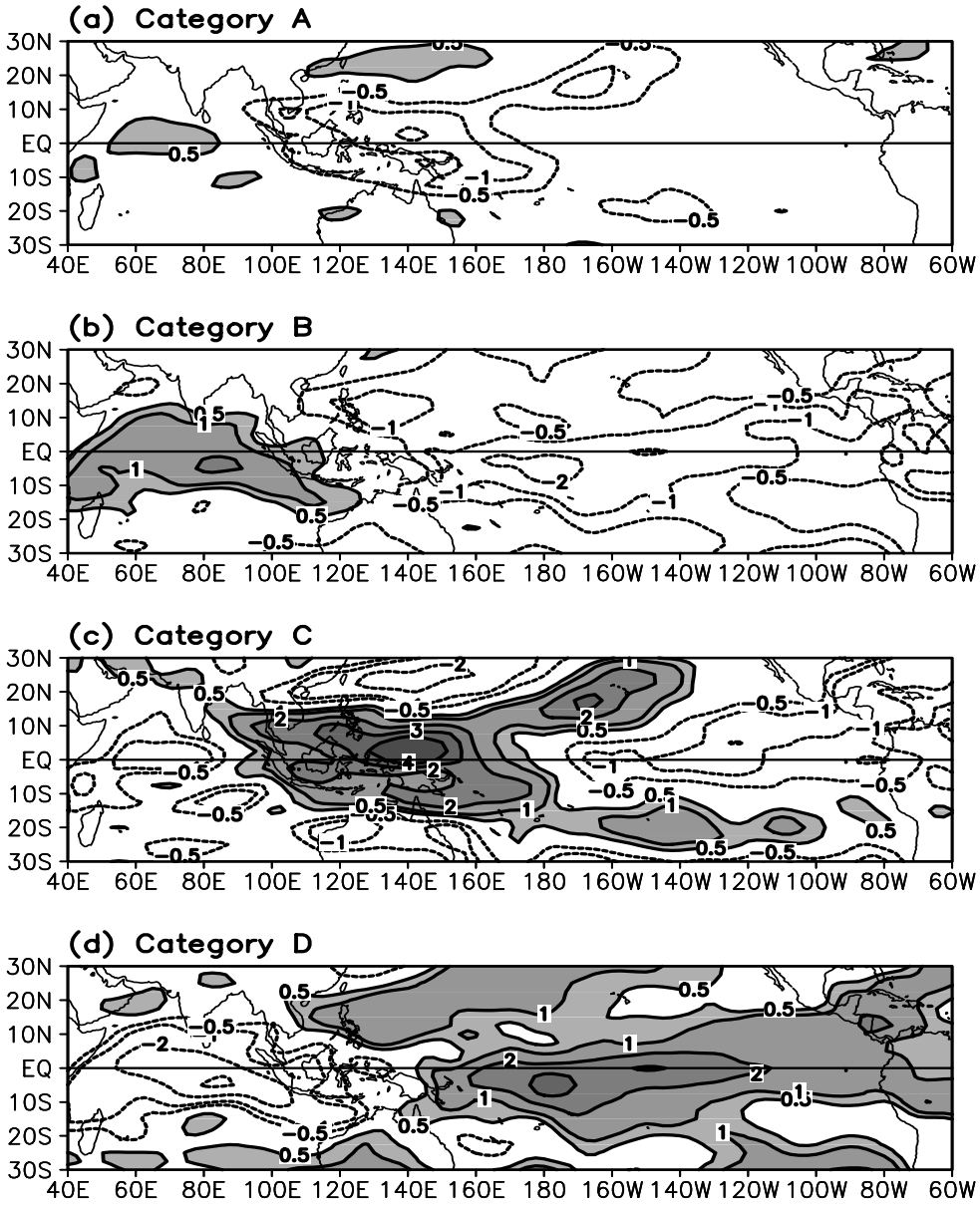

Fig. 8. Westerly wind anomalies, based on the regressed two leading SVD modes in each MJO category of (a) A, (b) B, (c) C, and (d) D. The contours are –3, –2, –1, –0.5, 0.5, 1, 2, 3 m s^{-1}; the zero contour is omitted, and the positive contours are shaded.

torially trapped eastward propagation.

The timing and position in longitude of TD/TCs in the Indian-western Pacific Oceans, those formed in the north/south of the tropical regions respectively labeled by N/S along with the six times of the MJO westerly wind burst are shown in Fig. 9. We can observe that most of the TD/TCs formed in both off-equatorial Indian-western Pacific sectors are concentrated in the period of October 1996 to the end of January 1997, and the period of April 1997 to the end of early June 1997, probably modulated by MJO b, c, e, and f. In these times, there are series of TD/TCs formed in a several- to ten-day interval in the downstream direction of the MJO westerly wind anomalies in both hemisphere tropical sectors. During the tropical cyclone seasons (summer to fall) in the north/south Indian-western Pacific Oceans, however, no such feature is found although there exists the eastward shift of MJO as we have observed in MJO a and d. Thus, there are more opportunities to generate tropical cy-

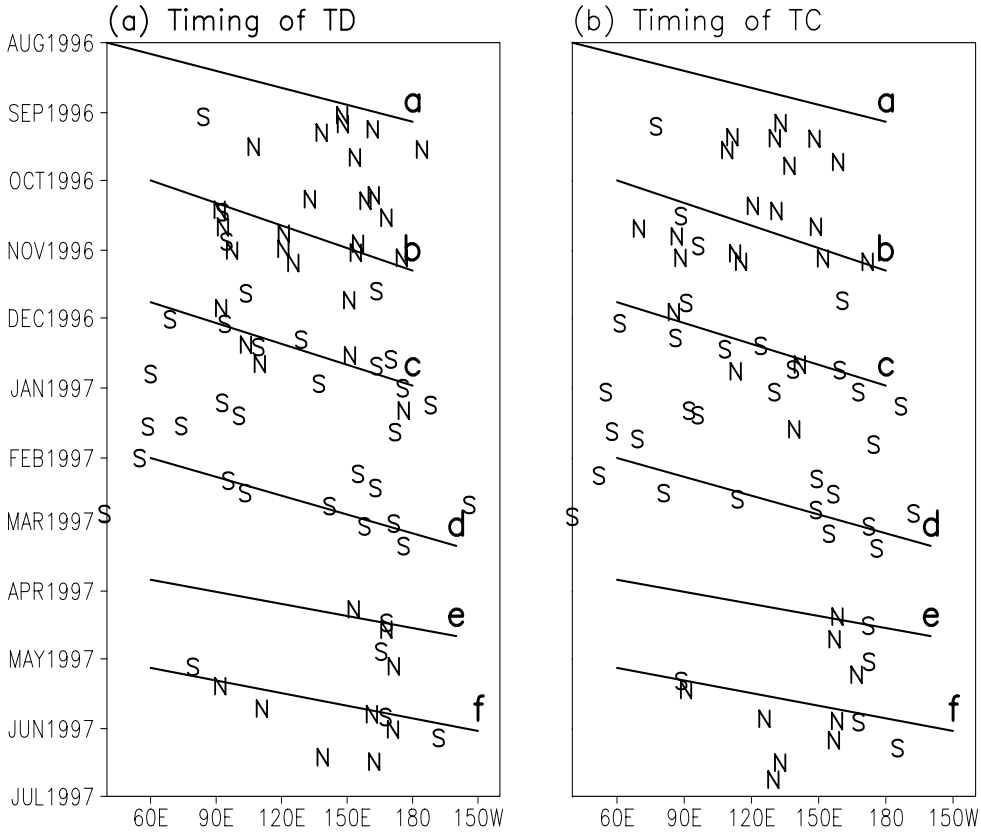

Fig. 9. Time-longitude cross-section of TD/TC positions along with the MJO westerly wind burst and its eastward propagation. (a) TD position in North/South Hemisphere marked by N/S; (b) TC position in North/South Hemisphere marked by N/S. a, b, c, d, e, and f denote each MJO event and its eastward propagation.

clones in the transition season than at other times.

Maps of TD/TC spatial distribution in the four MJO categories for each MJO event are shown in Fig. 10, which help us to distinguish the location and phase of possible twin tropical cyclone initial formation. In the figure, the label of A, B, C, and D is named after the MJO category in the same MJO event. We define that if the difference of location in longitude for twin tropical cyclones is less than 20 degrees, then we can find that two pairs of TDs labeled by A and B occurred in MJO-b in the tropical domain of the Indian Ocean. In the western Pacific, there is only one pair of TDs asymmetric about the equator around 160°E, labeled by D, which is probably influenced by the MJO westerly wind burst or westerly wind eastward propagation. In MJO-c, two pairs of TDs labeled by A and D respectively, are observed in the east of the Indian Ocean and at the western Pacific date line. In MJO-d, there is no pair of TDs found. Similarly, in MJO-e, there is only one pair of TDs, labeled by C, observed in the neighborhood of 170°E in the western Pacific. In MJO f, two pairs of TDs, labeled by A and C, that respectively formed in the Indian and western Pacific Oceans are found. In general, during period of 1 September 1996 to 30 June 1997, there are four pairs of TDs in the opposite equatorial Indian Ocean, probably modulated by the MJO westerly wind burst, and four pairs of TDs in the western Pacific Ocean.

As we have discussed the average period of MJO in each category is about 12 days, therefore there exists a several- to ten-day difference in TD formation, and those pairs of TDs should not be exactly defined as twin tropical cyclones. To accurately find the twin tropical cyclones probably modulated by the MJO westerly wind burst, we propose the concept of the twin tropical cyclone as a pair of tropical cyclones originating from the tropical depression, symmetric to one another about the equator in the Indian-western Pacific sectors within two days of difference in time of occurrence and 20 degrees difference of location in longitude under the same MJO wet phases. In the Indian Ocean, the phases are MJO categories A and B, and

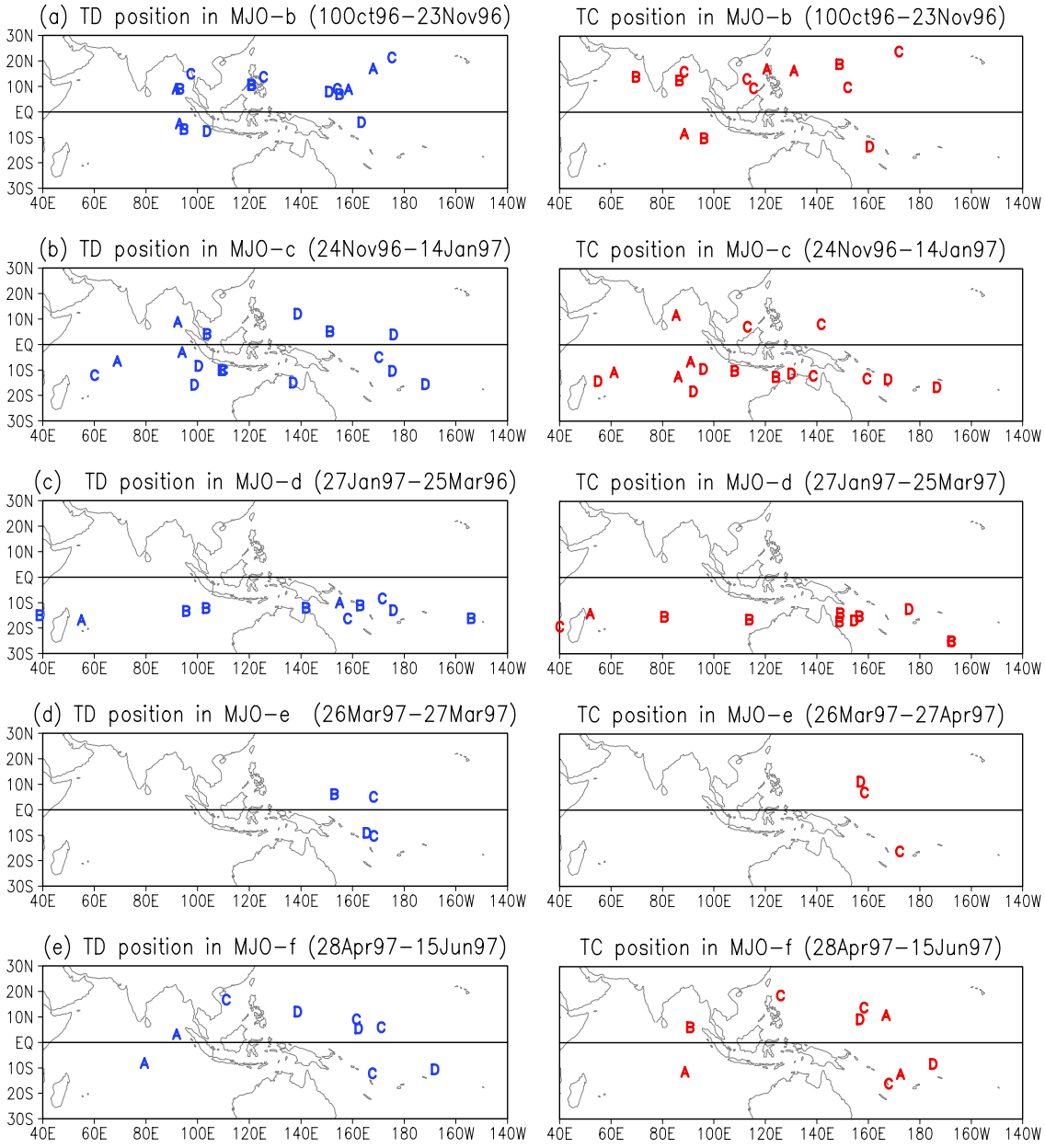

Fig. 10. Maps of TD (left panel) and TC (right panel) distribution in each MJO event of (a) MJO-b, (b) MJO-c, (c) MJO-d, (d) MJO-e, and (e) MJO-f. The time period for each MJO event is printed in the brackets of the title lines.

in the western Pacific, are MJO categories C and D. In the framework of this concept, two pairs of twin cyclones related with the MJO westerly wind burst are selected: one is in the Indian Ocean formed in the middle of October 1996 and modulated by MJO category A; the other is in the western Pacific, occurring in late May 1997 which is modulated by MJO category C.

Figure 11 shows these twin tropical best cyclone tracks and maximum wind speed. In the Indian Ocean, there is a couple of TDs: one is at about 9.1°N, 91.7°E, and was first recorded by JTWC at 0000 UTC 14 October; and the other is at about 4.6°S, 93.0°E, at 0000 UTC 15 October 1996. Both appear westward: shiffed after TD formation, and develop a tropical storm at 14.0°N, 69.7°E around 0006 UTC 22 and at 8.4°S, 88.5°E around 0018 UTC 16. The north one lasts for about 16 days, but the south one lasts only for 8 days, before their decay. In the western Pacific, there is a couple of TDs observed: one at about 9.1°N, 161.4°E at 0012 UTC 25 May 1997, and the other at about

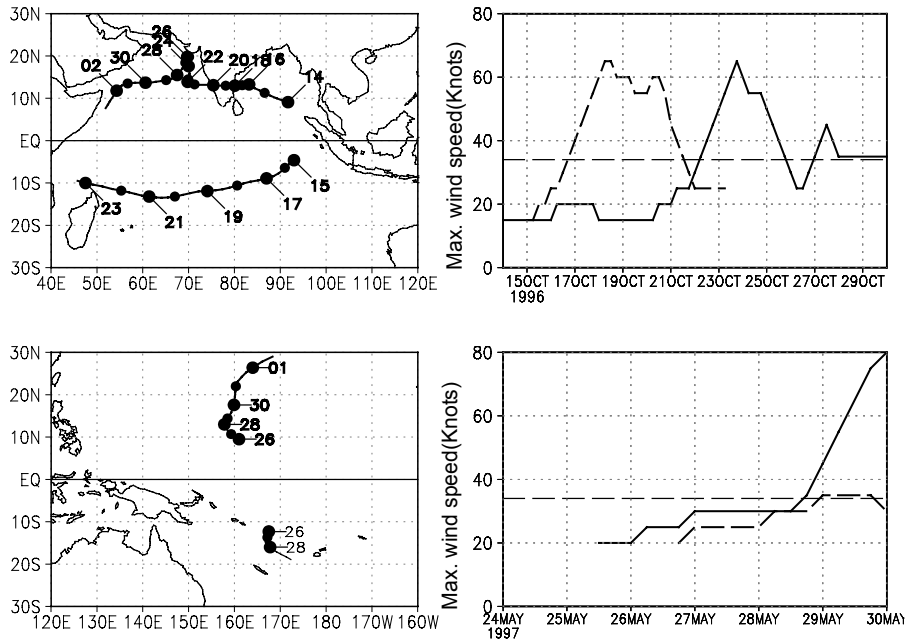

Fig. 11. Best track and maximum wind speed (knots) of twin cyclones observed in the Indian Ocean in October 1996 (upper panels) and in the western Pacific Ocean in May 1997 (lower panels). The maximum wind speed of TC in the Northern Hemisphere is indicated by the solid line. The numerical label in the best track denotes the TC position in the day at 0000 UTC.

12.1°S, 158.2°E at 0018 UTC May. Both exhibit poleward movement after the TD stage, and develop into tropical storm intensity at 14.0°N, 158.2°E around 0018 UTC 28 May, and at 16.0°S, 167.8°E around 0000 UTC 29 May respectively. The north one lasts for about 7 days, and the south one lasts for only 3 days, before their decay.

To trace the developing process of twin tropical cyclogenesis modulated by the MJO westerly wind burst, the temporal-spatial evolution of the daily wind vectors at 850 hPa and the GMS IR temperature, starting from 2 days earlier than the TD first record by JTWC, are shown in Fig. 12.

A couple of cyclonic flows and westerly wind along the equator is observed in the range of 60°E to 100°E in the Indian Ocean on 12 October, with the organized super cloud cluster in the downstream sectors of the westerly wind burst. On 13 October, the observed cyclonic vortices move westward, and the large area of the super cluster starts to break up and separates into two clusters: one around the equatorial sector, the other left in the south. On 14 October, a clear vortex forms in the North Indian Ocean around 90°E, and another vortex forms in the close south equatorial sector, both connected to each other by a stronger westerly wind and enhanced cloud convective cluster. On 15 October, a pair of isolated vortices asymmetric about the equator forms in the Indian Ocean with an independent cloud cluster although both are still linked by the enhanced westerly wind, suggesting that a real twin tropical cyclone has formed. In the following four days (from 16 to 19 October), the pair of tropical cyclone exhibits a westward shift, and the westerly wind is strongly enhanced and dominates the equatorial sectors for several days in the Indian Ocean with the intensified twin cyclones.

In the western Pacific around 22 May 1997, 3 days prior to the TD formation announced by JTWC (see Fig. 13), there is cyclonic flow along with the equatorial westerly wind burst and a convective cluster is observed around the domain of 130°E to 150°E in the tropical western Pacific region. In the south of the equator, however, no similar flow is found until 25 May, when the observed vortex in the north associated with the westerly wind moves eastward to 160°E, then a clear vortex-like flow forms in the south, which is connected to the north one by the enhanced westerly wind and well-organized cloud convective cluster. On 26 May, a real pair of tropical cyclones is found around 160°E close to the equator, and the cloud cluster starts to separate. On 27 May, the vortex pairs start to shift poleward, and a clear pair of cloud convective clusters are observed corresponding to each cyclonic vortex. However, in the following two days, the south vortex

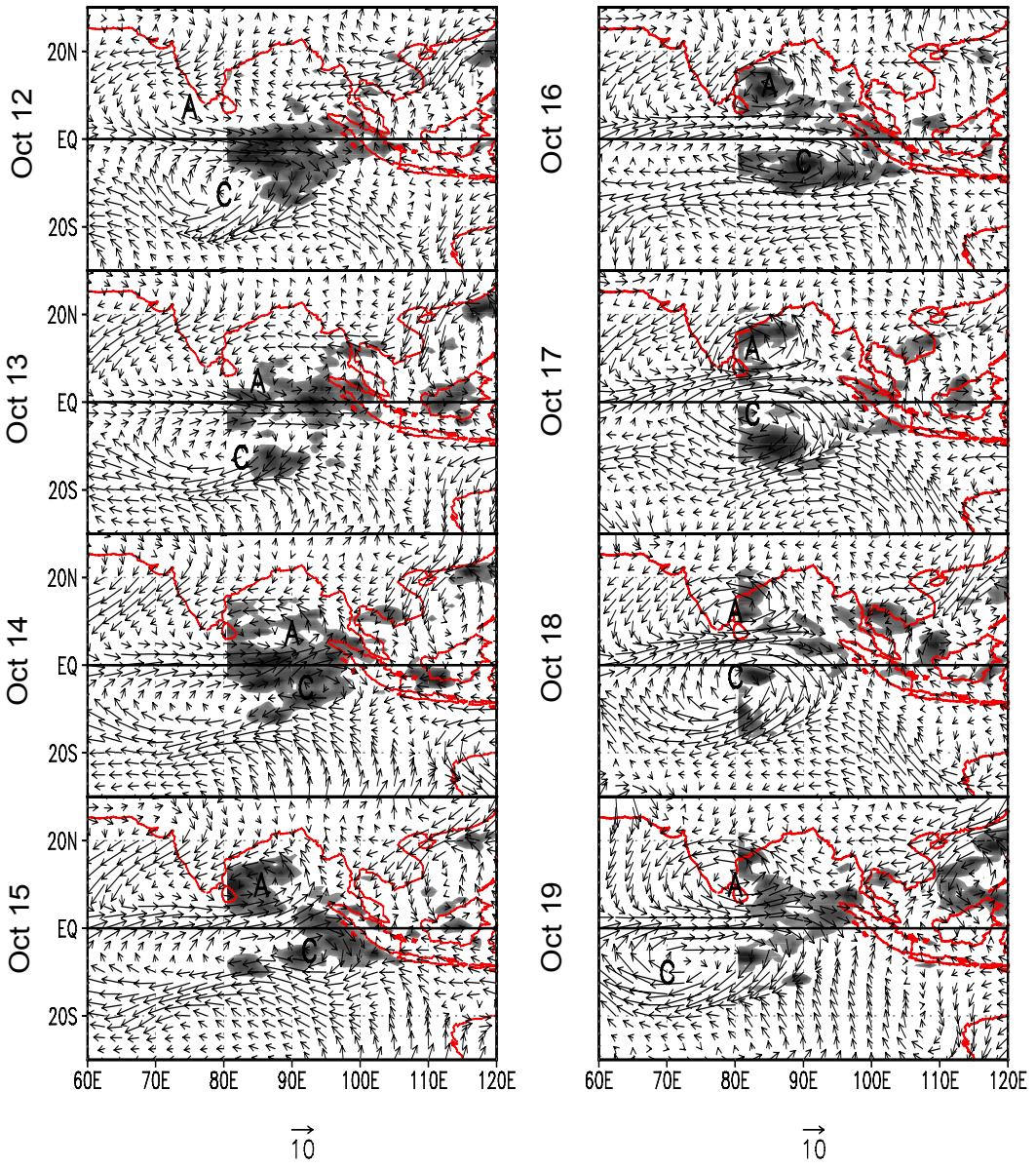

Fig. 12. Temporal-spatial evolution of daily 850-hPa wind vectors (m s^{-1}) and the GMS IR temperature-indicated cloud clusters (°C) for the observed twin cyclones in the Indian Ocean from 12 October 1996 to 19 October 1996. The time is indicated on the left-hand of the picture, and the shading denotes where the region of GMS IR temperature is less than –20°C. The A and C denote the anti-clockwise and clockwise vortices.

begins to decay with the cloud cluster away from the vortex center, in contrast with the developed tropical cyclone in the north.

As we have discussed above, the MJO westerly wind burst and its associated convection can result in a series of TC genesis in the Indian-western Pacific Oceans. However, the twin tropical cyclone, probably modulated by the MJO, is usually observed in the transition season, and pairs of TCs are observed in both tropical sectors of the Indian-western Pacific Oceans. Two remarkable twin tropical cyclogeneses probably modulated by the MJO westerly wind burst are found: one is observed in the Indian Ocean in the middle of October 1996, and the other is observed in the Western Pacific Ocean in late May 1997. The twin tropical cyclogenesis in mid-October 1996 is observed when the super cloud cluster is separated into two isolated clusters by the enhanced westerly wind, which is

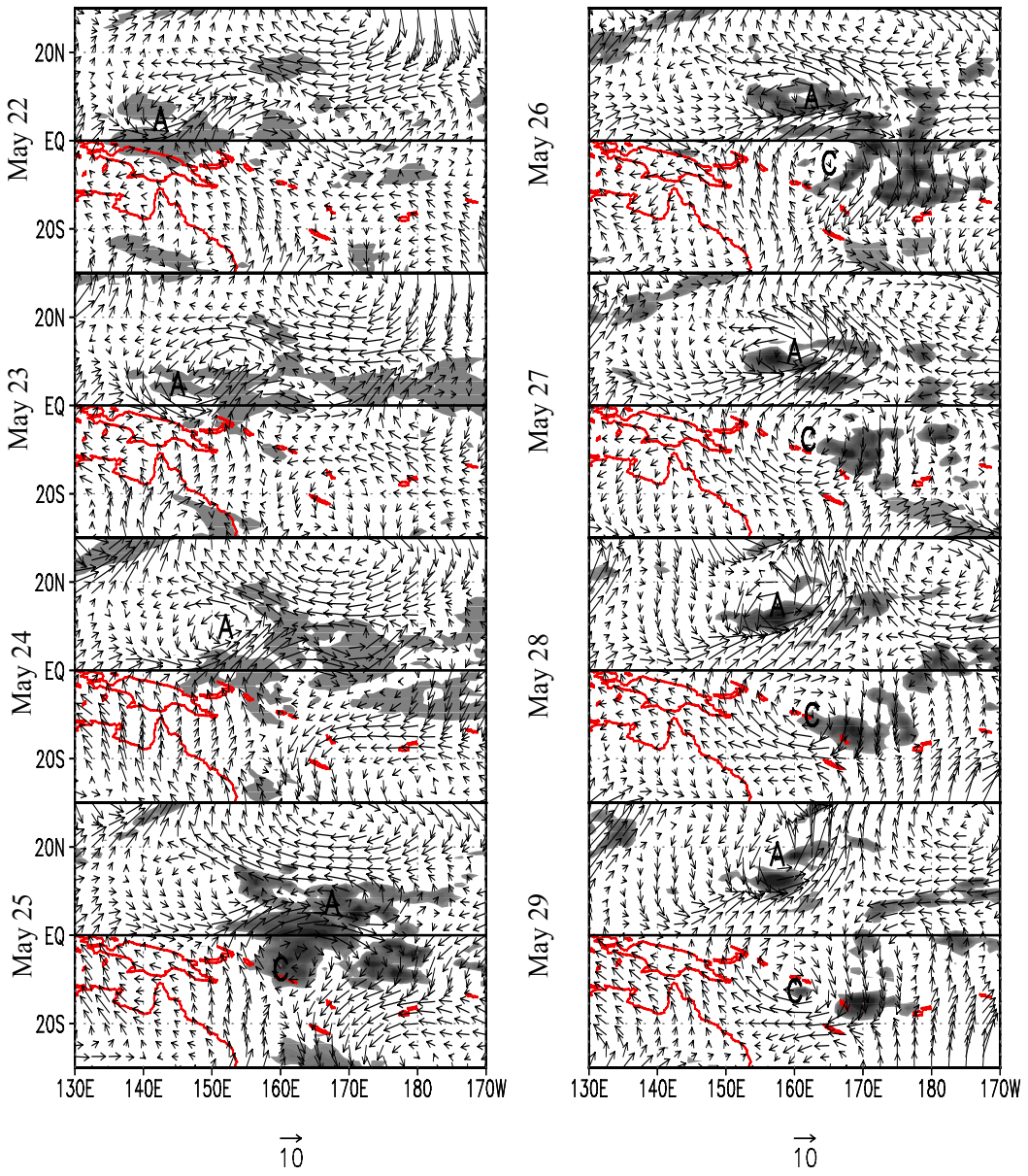

Fig. 13. Temporal-spatial evolution of daily 850-hPa wind vectors (m s^{-1}) and the GMS IR temperature-indicated cloud clusters (°C) for the observed twin cyclone in the western Pacific Ocean from 22 May 1997 to 29 May 1997. The time is indicated on the left-hand of the picture, and the shading denotes where the region of GMS IR temperature is less than –20°C. The A and C denote the anti-clockwise and clockwise vortices. respectively.

accompanied by two independent vortices in the equatorial tropical sectors. The other one, in late-May 1997, is characterized by one cyclonic flow that later results in another cyclonic cell in its opposite equatorial sector. Thus, there are two very important conditions for twin cyclogenesis: one is the MJO westerly wind straddling the equator, and the other is the integral super cloud cluster which splits into two cloud convective clusters with independent vortices.

After twin tropical cyclone genesis, both vortices begin west ward and poleward movement, in contrast to the eastward-shifting MJO super cloud cluster, which looks like the cloud cluster within a super cloud cluster demonstrated by Nakazawa (1988). Modeling study (Chao and Deng, 1998) suggests that an integral part of super cloud clusters, the westerly wind burst, is due to two or more successive cloud clusters pairs (vortex pairs, or twin cyclones) straddling the equator

that are generated by a cloud cluster tele-induction mechanism; when SST is not symmetric with respect to the equator, vortices may occur in one hemisphere only, but that is sufficient to give rise to the westerly wind bursts. Observation shows that the westerly wind burst is always associated with the earlier large scale vortex-like flow and super cloud cluster, but the twin cyclone and vortex pairs form when the super cloud cluster is separated into two isolated parts straddling the equator associated with each independent vortex. In additional, more observational and modeling studies have shown that the low-level cyclonic vorticity anomaly arises as an equatorial Rossby wave response to the anomalous MJO convective heating over Indonesia (Hedon and Salby, 1994; Matthews et al., 1999; Matthews, 2000). Thus, the MJO westerly wind burst is only one initial condition for the twin cyclone genesis; the super cloud cluster straddling the equator and finally separating into two isolated parts by the enhanced westerly wind corresponding to each independent vortex is another important condition for twin cyclone formation. During the transition season, because the ITCZ is close to the equator, there is more active convection in these sectors, modulated by the MJO westerly wind burst, therefore more twin cyclones can be observed compared with other seasons.

4. Concluding remarks

Following the way of Matthews (2000) and based on the analysis of Nakazawa (2000a, 2000b), the observational relationship between twin tropical cyclogenesis in the Indian-western Pacific Oceans and the MJO is explored focusing on the eastward propagating MJO shown by the first two EOF modes of band-pass filtered OLR.

We divide the MJO cycle into four categoris (A–D), and a westward propagating MJO category. In the Indian Ocean, the wet (dry) MJO phase is classed into categories A and B (C and D); in the northwestern Pacific, the wet (dry) MJO phase is classed into categories B and C (A and D); and in the southwestern Pacific, the wet (dry) phases of MJO occur in C and D (A and B).

The MJO westerly wind burst associated with its eastward propagation can result in a series of tropical cyclogeneses in a multi-day interval. Only in the transition seasons, pairs of TCs are observed in both tropical sectors of the Indian-western Pacific Oceans. Two remarkable twin tropical cyclogeneses probably modulated by the MJO westerly wind burst are found: one is observed in the Indian Ocean in the middle of October 1996, and the other is observed in the Western Pacific Ocean in late May 1997. The twin tropical cyclogenesis in mid-October 1996 is observed when the super cloud cluster is separated into two isolated clusters by the enhanced westerly wind, which is accompanied by independent vortices in the equatorial tropical sectors. The other one, in late May 1997, is characterized by one cyclonic flow that later results in another cyclonic cell in its opposite equatorial sector. Thus, there are two very important conditions for twin cyclogenesis: one is the MJO westerly wind straddling the equator, and the other is the integral super cloud cluster, which splits into two cloud convective clusters with independent vortices.

Acknowledgments. This work was supported by the CATT, Japan; the Scientific Research Foundation for the Returned Overseas Chinese Scholars, State Education Ministry; and LASG, Institute of Atmospheric Physics, Chinese Academy of Sciences. The authors wish to thank Dr. Yuhji Kuroda and Dr.Yoshimura who supplied the EOF and SVD source codes, Dr. Mitsuru Ueno and Dr. Hirotaka Kamahori for useful discussion, and Mr. Kiyotoshi Takahashi for preparing the GMS IR data. The wavelet software was provided by C.Torrence and G. Compo, and is available at the URL: http://paos.colordo.edu/research/wavelets/.

REFERENCES

Chao, W. C., and L. Deng, 1998: Tropical intraseasonal oscillation, super cloud cluster, and cumulus convection schemes. Part II: 3D Aquaplanet simulations. *J. Atmos. Sci.*, **25**, 690–709.

Evans, J. L., and R. J. Allan, 1992: El Niño/Southern Oscillation modification to the structure of monsoon and tropical cyclone activity in the Australian region. *Int. J. Climatol.*, **12**, 611–623.

Gray, W. M., 1979: Hurricanes: Their formation, structure and likely role in the tropical circulation. *Meteorology over the Tropical Oceans*, D. B. Shaw, Ed., *Roy. Meteor. Soc.*, 155–218.

Hall, J. D., A. J. Matthews, and D. J. Karoly, 2001: The modulation of tropical cyclone activity in the Australian region by the Madden-Julian Oscillation. *Mon. Wea. Rev.*, **129**, 2970–2982.

Hendon, H. H., and M. L. Salby, 1994: The life cycle of the Madden-Julian Oscillation. *J. Atmos. Sci.*, **51**, 2225–2237.

Hendon, H. H., and B. Liebmann, 1994: Organization of convection within the Madden Julian Oscillation. *J. Geophys. Res.*, **99**, 8073–8083.

Kalnay, E., and Coauthors, 1996: The NCEP/NCAR 40-year reanalysis project. *Bull. Amer. Meteor. Soc.*, **77**, 437–471.

Kiladis, G. N., and K. M. Weickmann, 1992: Circulation anomalies associated with tropical convection during northern winter. *Mon. Wea. Rev.*, **120**, 1900–1923.

Knutson, T. R., and K. M. Weickmann, 1987: 30-60 day atmospheric oscillations: Composite life cycles of convection and circulation anomalies. *Mon. Wea. Rev.*, **115**, 950–972.

Kuroda, Y., 1998: An effective SVD calculation method for climate analysis. *J. Meteor. Soc. Japan*, **76**, 649–655.

Lau, K. M., P. Li, C. H. Sui, and T. Nakazawa, 1989: Dynamics of super cloud cluster, westerly wind bursts, 30–60 day oscillation and ENSO: An unified view. *J. Meteor. Soc. Japan*, **67**, 205–219.

Li Chongyin, and Wu Peili, 1990: An observational study of the 30–50 day atmospheric oscillations. Part I: Structure and propagation. *Advances in Atmospheric Sciences.*, **7**, 294–304.

Liebmann, B., H. H. Hendon, and J. D. Glick, 1994: The relationship between tropical cyclones of the western Pacific and Indian Oceans and the Madden-Julian Oscillation. *J. Meteor. Soc. Japan*, **72**, 401–411.

Madden, R. A., and P. R. Julian, 1971: Detection of a 40–50 day oscillation in the zonal wind in the tropical Pacific. *J. Atmos. Sci.*, **28**, 702–708.

Madden, R. A., and P. R. Julian, 1994: Observations of the 40–50 day tropical oscillation-A review. *Mon. Wea. Rev.*, **122**, 814–837.

Maloney, E. D., and D. L. Hartmann, 1999: Modulation of eastern North Pacific hurricanes by the Madden-Julian Oscillation. *J. Climate*, **13**, 1451–1460.

Maloney, E. D., and D. L. Hartmann, 2000: Modulation of hurricane activity in the Gulf of Mexico by the Madden-Julian Oscillation. *Science*, **287**, 2002–2004.

Matthew, A. J., J. M. Slingo, B. J. Hoskins, and P. M. Inness, 1999: Fast and slow Kelvin waves in the Madden-Julian oscillation of a GCM. *Quart. J. Roy. Meteor. Soc.*, **125**, 1473–1498.

Matthew, A. J., 2000: Propagation mechanisms for the Madden-Julian Oscillation. *Quart. J. Roy. Meteor. Soc.*, **126**, 2637–2652.

McPhaden, M. J., 1999: Climate oscillations–Genesis and evolution of the 1997–98 El Niño. *Science*, **283**, 950–954.

Murakami, T., L.-X. Chen, and A. Xie, 1986: Eastward propagation of 30–60 day perturbations as revealed from OLR data. *J. Atmos. Sci.*, **43**, 961–971.

Nakazawa, T., 1986: Intraseasonal variation of OLR in the tropics during the FGGE year. *J. Meteor. Soc. Japan*, **64**, 17–34.

Nakazawa, T., 1988: Tropical super clusters within intraseasonal variations over the western Pacific. *J. Meteor. Soc. Japan*, **66**, 823–839.

Nakazawa, T., 2000a: MJO and tropical cyclone activity during 1997/98 ENSO. *Adv. Space Res*, **25**, 953–958.

Nakazawa, T., 2000b: Suppressed tropical cyclone formation over the western North Pacific in 1998. *J. Meteor. Soc. Japan*, **79**, 173–183.

Nakazawa, T., and C. Zhu, 2001: Estimation of typhoon position and intensity from NSACT data. Workshop on Typhoon Forecasting Research, Seogwipo-si, Jejudo, Korea, Ed. ESCAP/WMO Typhoon Committee, 138–140.

Ogura, Y., and H.-N. Chin, 1987: A case of cross-equatorial twin vortices over the Pacific in the Northern winter using FGGE data. *J. Meteor. Soc. Japan*, **65**, 669–674.

Reynolds, R. W., and T. M. Smith, 1994: Improved global sea surface temperature analyses. *J. Climate*, **7**, 929–948.

Rui, H., and B. Wang, 1990: Development characteristics and dynamic structure of tropical intraseasonal convective anomalies. *J. Atmos. Sci.*, **47**, 357–379.

Solow, A., and N. Nicholls, 1990: The relationship between the Southern Oscillation and tropical cyclone frequency in the Australian region. *J. Climate*, **3**, 1097–1101.

Slingo, J. M., and coauthors, 1999: On the predictability of interannual behavior of Madden-Julian Oscillation and its relationship with El Niño. *Quart. J. Roy. Meteor. Soc.*, **125**, 583–609.

Zehr, R. M., 1992: Tropical cyclogenesis in the western North Pacific. NOAA Tech. Rep. NESDIS **61**, 2–3.